EUROPEAN ORGANIZATION FOR NUCLEAR RESEARCH

Proposal to the ISOLDE and Neutron Time-of-Flight Committee

Laser Spectroscopy of neutron-deficient Sn isotopes

January 11, 2016

R.F. Garcia Ruiz[1], D.L. Balabanski[2], C.L Binnersley[1], J. Billowes[1], M.L. Bissell[1], K. Blaum[3], T.E. Cocolios[4], R.P. de Groote[4], G.J. Farooq-Smith[4], K.T. Flanagan[1], S. Franchoo[5], G. Georgiev[6], A. Koszorús[4], M. Kowalska[7], K.M. Lynch[8], S. Malbrunot-Ettenauer[8], B.A. Marsh[9], E. Minaya Ramirez[5], P. Naubereit[10], G. Neyens[4], W. Nörtershäuser[11], S. Rothe[1], R. Sánchez[12], H.H. Stroke[13], D. Studer[10], A.R. Vernon[1], K.D.A. Wendt[10], S.G. Wilkins[1], Z. Xu[4], X.F. Yang[4], D.T. Yordanov[5]

[1]*School of Physics and Astronomy, The University of Manchester, Manchester, M13 9PL, UK*
[2]*ELI-NP, IFIN-HH, 077125 Magurele, Romania*
[3]*Max-Planck-Institut für Kernphysik, D-69117 Heidelberg, Germany*
[4]*KU Leuven, Instituut voor Kern- en Stralingsfysica, B-3001 Leuven, Belgium*
[5]*Institut de Physique Nucleaire Orsay, IN2P3/CNRS, 91405 Orsay Cedex, France*
[6]*CSNSM, CNRS-IN2P3, Université Paris-Sud, F-91405 Orsay, France*
[7]*Experimental Physics Department, CERN, CH-1211 Geneva 23, Switzerland*
[8]*Physics Department, CERN, CH-1211 Geneva 23, Switzerland*
[9]*Engineering Department, CERN, CH-1211 Geneva 23, Switzerland*
[10]*Institut für Physik, Johannes Gutenberg-Universität, D-55128 Mainz, Germany*
[11]*Technische Universität Darmstadt, 64289 Darmstadt, Germany*
[12]*GSI Helmholtzzentrum für Schwerionenforschung GmbH, D-64291 Darmstadt, Germany*
[13]*Department of Physics, New York University, New York, New York 10003, USA*

Spokesperson:[Ronald Garcia Ruiz] [ronald.fernando.garcia.ruiz@cern.ch]
Contact person:[Kara M. Lynch] [kara.marie.lynch@cern.ch]

CERN-INTC-2016-006 / INTC-P-456
11/01/2016

Abstract: We propose to study the ground state properties of neutron-deficient tin isotopes towards the doubly-magic nucleus ^{100}Sn. Nuclear spins, changes in the rms charge radii and electromagnetic moments of $^{101-121}$Sn will be measured by laser spectroscopy using the CRIS experimental beam line. These ground-state properties will help to clarify the evolution of nuclear structure properties approaching the $N = Z = 50$ shell closures. The tin isotopic chain is currently the frontier for the application of state-of-the-art ab-initio calculations. Our knowledge of the nuclear structure of the Sn isotopes will set a benchmark for the advances of many-body methods, and will provide an important test for modern descriptions of the nuclear force.

Requested shifts: 35 shifts distributed in 2 runs.

1 Motivation

The persistent interest in the region around $N = Z = 50$ has been a strong motivator for the development of diverse experimental and theoretical studies in recent years [1, 2, 3, 4, 5]. In addition to the importance for nuclear structure, our understanding of nuclei in the neighborhood of the heaviest self-conjugate doubly-magic nucleus, $^{100}_{50}\mathrm{Sn}_{50}$, has relevance also for our knowledge of astrophysics, as this region is considered to be the end of the rapid-proton (rp) capture process [6].

Contradictory experimental evidence has been reported about the level ordering of shell-model orbits in the neutron deficient Sn isotopes [7, 8], and several questions remain open in connection with the robustness of the $N = Z = 50$ shell closures [9, 10, 6]. While the greatest Gamow-Teller strength found in ^{100}Sn supports a shell-model picture with strong $N = Z = 50$ shell closures [6], the existence of low-lying energy levels and relatively large $B(E2)$ values (known down to ^{104}Sn [3, 10, 11]) points to a rather weak ^{100}Sn core. To provide quantitative arguments to this debate, the current proposal aims to answer two pressing questions of nuclear structure in this region: to what extent can our simplified single particle picture be applied to the description of Sn isotopes, and what is the influence of the microscopic treatment of the nuclear force in the description of such a complex nuclear many-body problem.

Currently, laser-spectroscopy experiments on Sn isotopes have been performed only down to ^{108}Sn [12, 13, 14]. This proposal aims to extend these measurements down to ^{101}Sn ($N = 51$), providing direct assignments for the ground state (gs) spins and high-precision measurements of ground state electromagnetic moments and changes in the rms charge radii, which are essential to understand the evolution of nuclear structure around $N = Z = 50$.

1.1 Spins and electromagnetic moments

With the assumption of a doubly-magic ^{100}Sn nucleus, the description of ^{101}Sn is expected to be dominated by a single-neutron in the $\nu d_{5/2}$ (or $\nu g_{7/2}$) orbit. The shell-model orbitals above ^{100}Sn are shown in Figure 1. Previous decay studies supported the "normal" shell-model ordering in neutron-deficient isotopes, with the orbit $\nu d_{5/2}$ dominating their ground state [7]. This description was contradicted by later experiments, suggesting an inversion of the $\nu d_{5/2}$-$\nu g_{7/2}$ orbits around ^{101}Sn [8]. Direct spin assignments, together with magnetic moment measurements to probe the wave function configuration of the ground state of $^{101-107}$Sn, are necessary to unambiguously determine the ordering of the $\nu d_{5/2}$-$\nu g_{7/2}$ orbits.

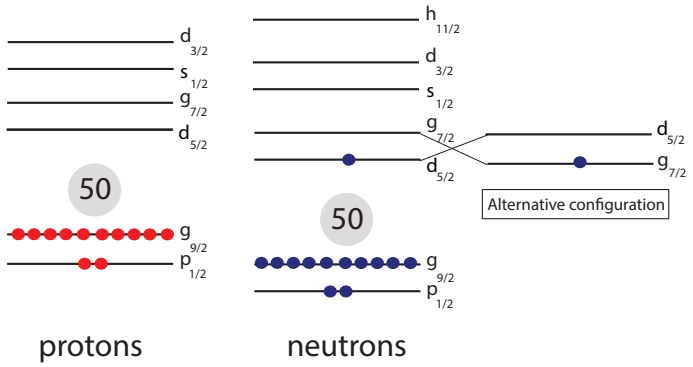

Figure 1: Shell-model orbitals assumed for the nucleus ^{101}Sn.

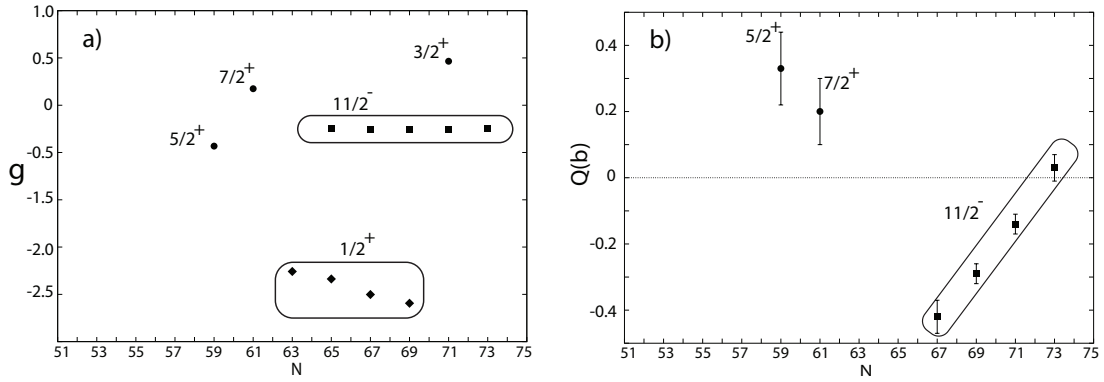

Figure 2: Experimental literature values for the g-factors ($g = \mu/(\mu_N I)$) (left) and quadrupole (right) moments of Sn isotopes as a function of the neutron number [16]. The electromagnetic-moments for the ground-state ($1/2^+$) and the isomeric states ($11/2^-$) display simple trends interpreted as dominant single-particle behavior. Below ^{115}Sn ($N = 65$) the experimental information on the quadrupole moments is rather poor and a firm conclusion cannot be drawn. The sign of the quadrupole moment for ^{119}Sn has not been measured, but was assumed to be negative, based on the systematic of the region.

The literature values for the ground state electromagnetic moments of Sn isotopes up to ^{123}Sn are shown in Figure 2. The remarkably simple trends observed for the neutron-rich isotopes suggests a dominant single-particle behaviour towards $N = 82$. Such mechanism has been advocated in neutron-rich Cd ($Z = 48$) isotopes [15]. For Sn isotopes it can be inferred from the fairly constant behaviour of the g-factors for the $1/2^+$ (ground) and $11/2^-$ (isomer) states (Figure 2a), and the linear trend observed in the quadrupole moments of the isomers, which is typical for seniority-two configurations filling gradually an orbital (Figure 2b). Thus, whether or not this simple single-particle like behaviour persists in the proximity of $N = Z = 50$ remains as an open question. While experimental evidence points to the existence of a dominant single-particle behavior towards $N = Z = 50$ [7, 6], complementary studies suggested a collective behavior dominated by multiple particle-hole excitations [10, 11, 8]. Electromagnetic moments are very sensitive to the details of the nuclear wave function, and if present, to the type of configuration mixing [17]. The extension of these measurements to neutron-deficient Sn isotopes will provide a unique scenario to quantify the importance of cross-shell excitations around $N = Z = 50$. This proposal will provide the first experimental determination of the ground state moments of $^{101-107}$Sn isotopes, shedding light on the role of core excitations around ^{100}Sn. This has recently been suggested from Coulomb excitation experiments [3, 4] and supported by large scale shell-model calculations using both realistic interactions [5] and valence-space interactions derived from chiral effective field theory [2]. Therefore, these measurements will provide an important test for these newly developed theoretical calculations. Additionally, firm spin assignments to $^{101-107}$Sn isotopes will be obtained to determine the ordering of the shell-model orbitals in this region.

Concerning isomers, there is only one known in the neutron-deficient Sn region, ^{113m}Sn ($7/2^+$, $T_{1/2} = 21.4$ m), whose electromagnetic properties are unknown, with different nature to the other isomers in the tin isotopic chain ($11/2^-$). It has previously been demonstrated that laser spectroscopy can reveal the existence of new nuclear states, e.g., for states of long lifetime that

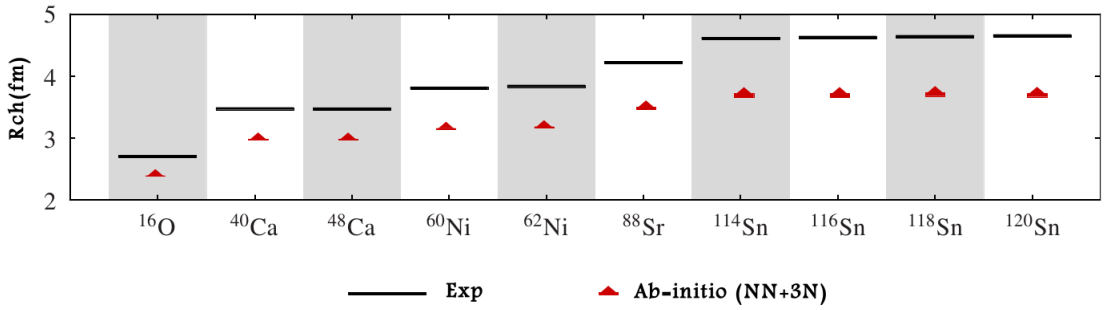

Figure 3: Experimental charge radii of different magic and semi-magic nuclei, compared with ab-initio calculations using the NN+3N chiral interaction [24]. The notable underestimation of charge radii has been a long-standing problem for the development of chiral Hamiltonians [23, 25].

can not be differentiated in decay spectroscopic methods [18].

1.2 Charge radii

The increasing effort in the description of inter-nucleon interactions derived from chiral effective field theory [19, 20] and the progress of many-body methods [21, 22] has opened the doors towards an ab-initio description of nuclear structure properties of medium mass and heavy nuclei, placing the Sn isotopes at the very front for the application of such ab-initio calculations [23].
Figure 3 shows a set of ab-initio calculations reported for the charge radii of several semi-magic isotopes up to ^{120}Sn [24]. Although, chiral Hamiltonians provide a relatively good description of binding energies [23], charge radii are significantly underestimated, and the discrepancies between theory and experiment increase with the mass number. This persistent underestimation of charge radii has been a long-standing problem for the development of chiral Hamiltonians. A recent effort to overcome this difficulty has led to a revised parametrization of the nuclear force [25]. The resulting interaction has provided a relatively good description of charge radii up to Ca isotopes [26, 27]. Work is in progress to extend these calculations to the Sn isotopes [28]. Additionally, it has been shown that the charge radii are sensitive to new aspects of nuclear structure [27], providing a powerful test to ab-initio methods, DFT approaches and shell-model calculations.

2 Experimental details

The ground-state properties will be obtained from measurements of the hyperfine structure spectra (hfs) and isotope shifts on the Sn ionic (or atomic) system by using the collinear resonance ionization laser spectroscopy experiment (CRIS) at ISOLDE [29, 30]. The HRS separator will be used in combination with the cooler-buncher ISCOOL. Bunches of singly-ionized Sn ions (Sn II) will be redirected into the CRIS beam line. In cases where the atomic state is preferred, the ions can be neutralized by using a charge exchange cell (CEC). At CRIS, the ions (or atoms) overlap with a laser beam in a collinear geometry along a UHV interaction region (1.2 m) to step-wise excite and ionize either the atomic state (Sn I) into the Sn II state, or the Sn II state

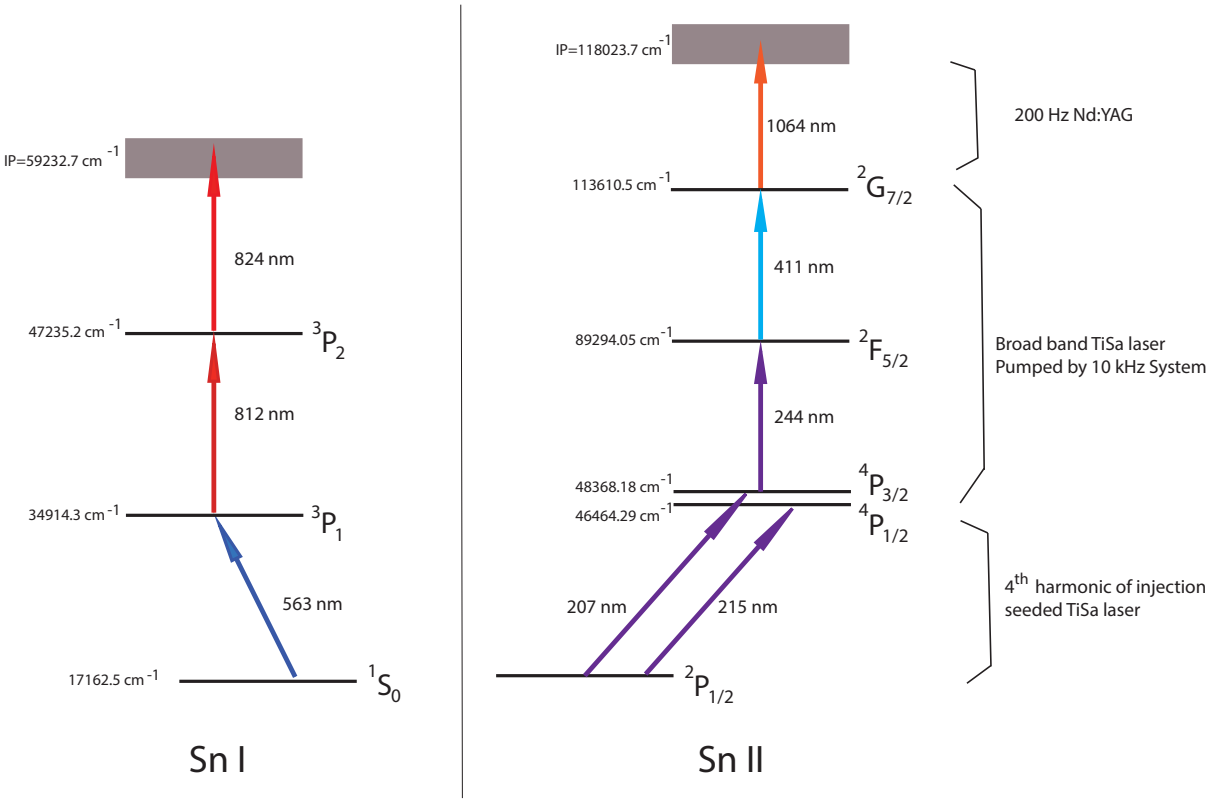

Figure 4: Resonance ionization schemes proposed for the study of Sn isotopes. Alternative to the atomic transitions (left), the ionic transition (right) can be used which could potentially provide higher sensitivity [31].

into the Sn III state. The resonantly-ionized ions are then separated from the non-interacting atoms (or from the singly-charged ions) via electrostatic deflector plates and detected by an MCP particle detector, thus reducing significantly the background in such experiments.
Several atomic transitions have been used in previous laser spectroscopy experiments of Sn isotopes [12, 13, 14]. These transitions have been well studied, and have proved to be sensitive to the nuclear spins, gs electromagnetic moments and changes in the rms charge radii. Although the aims of this proposal can be accomplished by using the atomic transition $5s^2\ 5p^2\ ^1S_0 \rightarrow 5p\ 6s\ ^3P_1$ [13], higher sensitivity could potentially be achieved by using the ionic system, Sn II (Figure 4). An offline plasma source has been installed at CRIS to investigate the feasibility of these Sn II transitions. Moreover, thanks to considerable investment from the FWO, STFC and ERC funding, the current CRIS laser lab has now the capability to study the two schemes presented in Figure 4.

The study of the Sn isotopes requires additional challenges for laser spectroscopy. Firstly, a relatively high contamination from Indium isobars is predicted for the most exotic neutron-deficient isotopes (see Figure 5), i.e., around 10^4 for mass $A = 102$ in comparison to a 10 yield for ^{102}Sn [32]. However, such contamination factors have been observed in other cases previously successfully studied at CRIS [33]. At current operating pressures ($\sim 10^{-8}$mbar) the nonresonant ionization efficiency is estimated to be less than 1:10^5 [33]. Therefore, the isobar yields will be reduced to less than 10 cps for ^{104}In, and less than 1 cps for ^{103}In. Furthermore, given the high

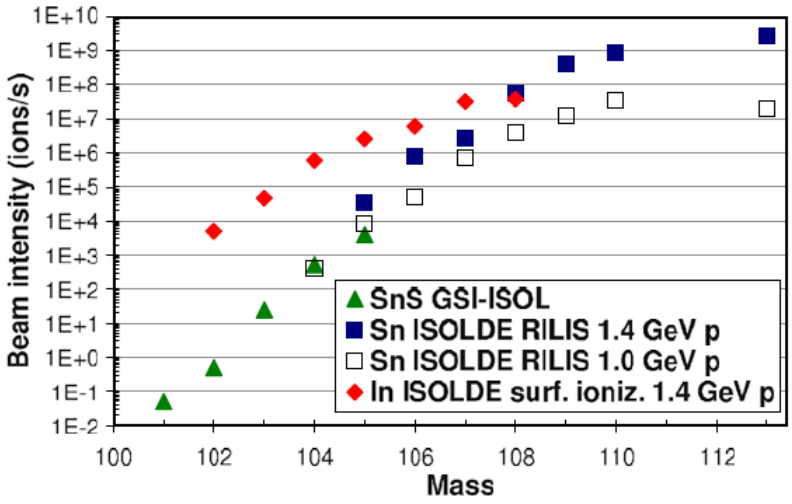

Figure 5: Beam intensities of neutron-deficient Sn isotopes measured as SnS^+ at GSI-ISOL and as Sn^+ with RILIS at ISOLDE from a LaC_x target. Figure taken from Ref. [32].

second ionization potential of In and Sn to produce doubly charged ions, 18.8 eV and 14.6 eV [31], respectively, the background associated with the collisional ionization-rate, which is the dominant source of background at CRIS, will be reduced by performing the hfs measurements on the Sn ionic system (Sn II). Thus, a further background reduction by a factor of ~ 1000 is expected for hfs spectra of the doubly-ionized Sn isotopes (Sn III) in comparision to performing ionization on the atomic state. Additionally, by using directly the ground state of the Sn ion avoids the use of the alkali vapour charge-exchange cell, improving the overall sensitivity and transmission efficiency of the CRIS measurements.
Secondly, the proposed low-lying transitions for Sn I and Sn II have low absorption cross sections [31, 34]. These "weak" transitions are an advantage for the CRIS technique as the relative long lifetimes of these low-lying excitation levels allow a complete time decoupling of the different laser pulses, eliminating possible coherent effects and the broadening induced by high intensity laser fields [35]. The high-resolution laser spectroscopy studies of Sn II require the use of narrow-band laser light with wavelengths in the range of the deep UV. In order to access such demanding wavelengths, the CRIS collaboration have acquired a complete new laser setup (see Sec. 2.1).

2.1 Laser setup

The resonance ionization scheme proposed for the study of Sn isotopes is shown in Figure 4. An injection seeded laser system has been recently installed at CRIS [36] to provide the narrow band laser light required for the resonance excitation step (207 nm). A new high power broad-band frequency quadrupled Ti:Sa laser setup (10 kHz), currently available in the CRIS laser lab, will be used to provide the second (244 nm) and the third steps (411 nm) from the second harmonic. The 1064 nm ionization step will be obtained from a high-power Nd:YAG laser (200 Hz), used during previous CRIS experiments [35].

Isotope	Half life	Estimated Yield (ions/s)	Target+RILIS	Shifts
^{101}Sn	0.86 s	$\sim$1	LaC_x	
^{102}Sn	3.8 s	$\sim10^1$	LaC_x	(Total: 15 shifts)
^{103}Sn	7.0 s	$\sim10^2$	LaC_x	
$^{104-113,113m}$Sn	$>$ 20 s	$\geq10^3$ (Ref. [32])	LaC_x	
^{117m,119m,121m}Sn	$>$ 40 min	$\geq10^7$	LaC_x	(Total: 15 shifts)
$^{114-124}$Sn	stable	$\geq10^7$	LaC_x	5

Table 1: Table of estimated yields and beam time request. Beam intensities correspond to 2 μA of average proton current at 1.4 GeV. For masses below $A = 104$, the beam intensities are estimated from the reported values for $^{104-113}$Sn [32] (see Figure 5).

3 Beam-time request

The high efficiency obtained by particle detection has allowed hyperfine-structure (hfs) measurements of low resolution at CRIS to be preformed on isotopes produced at rates of $\sim$100 ions/s. For the case of ^{202}Fr in 2012, whose yield has been $\sim$70 ions/μC, a clear hfs spectrum was obtained in a scan of only 2 hours [33, 37]. Recently, high-resolution measurements, down to 20(1) MHz [35], were accomplished on Fr isotopes by using a chopped cw laser beam in combination with a high intensity pulsed laser beam [35]. Such results, in combination with the ability to perform hfs at very low background conditions, [33] has opened the possibility to push the limits of sensitivity to study ions produced at rates of only few ions/s.

Since the experimental campaign in 2012, significant progress on the overall sensitivity and background reduction has been made at the CRIS beam line. New high-power and high-repetition-rate lasers systems have been acquired, and a second MCP detector setup has been installed to improve the efficiency of particle detection. Additionally, a new charge exchange cell is being developed to improve the ion beam transport and UHV in the interaction region, which will further reduce the non-resonant ionization background.

The details of the beam production and the required shifts for this experimental proposal are summarized in Table 1. The production of neutron-deficient Sn isotopes has been measured down to ^{104}Sn, whose yield was reported to be $\sim10^3$ ions/s using a LaC_x target with the resonance ionization ion source (RILIS) [32]. The yields for lighter Sn isotopes ($<^{104}$Sn) presented in Table 1 were estimated as an extrapolation from the reported values for $^{104-110}$Sn [32].

Summary of requested shifts: 35 shifts are required, distributed in two runs of 18 and 17 shifts, respectively.

References

[1] Faestermann, T., Górskab, M. & Grawe, H. *Prog. Part. Nucl. Phys.* **69**, 85–130 (2013).

[2] Bader, V. *et al. Phys. Rev. C* **88**, 051301(R) (2013).

[3] Doornenbal, P. *et al. Phys. Rev. C* **90**, 061302(R) (2014).

[4] Allmond, J. *et al. Phys. Rev. C* **92**, 041303(R) (2015).

[5] Coraggio, L. *et al. Phys. Rev. C* **91**, 041301(R) (2015).

[6] Hinke, C. *et al. Nature* **486**, 341–345 (2012).

[7] Seweryniak, D. *et al. Phys. Rev. Lett.* **99**, 022504 (2007).

[8] Darby, I. G. *et al. Phys. Rev. Lett.* **105**, 162502 (2010).

[9] Banu, A. *et al. Phys. Rev. C* **71**, 061305(R) (2005).

[10] Vaman, C. *et al. Phys. Rev. Lett.* **99**, 162501 (2007).

[11] Ekström, A. *et al. Phys. Rev. Lett.* **101**, 012502 (2008).

[12] Anselment, M. *et al. Phys. Rev. C* **34**, 1052 (1986).

[13] Eberz, J. *et al. Z. Phys.* **A326**, 121 (1987).

[14] Le Blanc, F. *et al. Phys. Rev. C* **72**, 034305 (2005).

[15] Yordanov, D. T. *et al. Phys. Rev. Lett.* **110**, 192501 (2013).

[16] Stone, N. J. *Atomic Data And Nuclear Data Tables* **90**, 75–176 (2005).

[17] Neyens, G. *Rep. Prog. Phys.* **66**, 633 (2003).

[18] Cheal, B. *et al. Phys. Rev. C* **82**, 051302(R) (2010).

[19] Epelbaum, E., Hammer, H.-W. & Meißner, U.-G. *Rev. Mod. Phys.* **81**, 1773–1825 (2009).

[20] Hammer, H.-W., Nogga, A. & Schwenk, A. *Rev. Mod. Phys.* **85**, 197 (2013).

[21] Hagen, G., Hjorth-Jensen, M., Jansen, G. R., Machleidt, R. & Papenbrock, T. *Phys. Rev. Lett.* **109**, 032502 (2012).

[22] Somà, V., Cipollone, A., Barbieri, C., Navrátil, P. & Duguet, T. *Phys. Rev. C* **89**, 061301 (2014).

[23] Binder, S., Langhammer, J., Calci, A. & Roth, R. *Phys. Lett. B* **736**, 119 (2014).

[24] Binder, S. Coupled-cluster theory for nuclear structure. *PhD Thesis. TU Darmstadt* (2014).

[25] Ekström, A. *et al. Phys. Rev. C* **91**, 051301 (2015).

[26] Hagen, G. *et al. Nature Physics* **Accepted** (2015).

[27] Garcia Ruiz, R. F. *et al. Nature Physics* **Accepted** (2016).

[28] Duguet, T. *Private communication* (2016).

[29] Cocolios, T. E. *et al. Nucl. Inst. Meth. B* **317**, 565 (2013).

[30] Cocolios, T. E. *et al. Nucl. Inst. Meth. B* **In press** (2016).

[31] Kramida, A., Ralchenko, Y., Reader, J. & Team, N. A. *NIST Atomic Spectra Database* **(version 5.3)**, http://physics.nist.gov/asd (2015).

[32] Köster, U. *et al. Nucl. Inst. Meth. B* **266**, 4229–4239 (2008).

[33] Flanagan, K. *et al. Phys. Rev. Lett.* **112**, 112503 (2013).

[34] Kurucz, R. L. *Atomic spectral line database* (http://www.cfa.harvard.edu/ampcgi/read_pac, 1995).

[35] de Groote, R. P. *et al. Phys. Rev. Lett.* **115**, 132501 (2015).

[36] Volker, S. Laser developments and high resolution resonance ionization spectroscopy of actinide elements. *PhD Thesis. University of Jyvskyl* (2015).

[37] Lynch, K. M. *et al. Phys. Rev. X* **4**, 011055 (2014).

Appendix

DESCRIPTION OF THE PROPOSED EXPERIMENT

The experimental setup comprises: (*name the fixed-ISOLDE installations, as well as flexible elements of the experiment*)

Part of the	Availability	Design and manufacturing
CRIS	☒ Existing	☒ To be used without any modification
[Part 1 of experiment/ equipment]	☐ Existing	☐ To be used without any modification ☐ To be modified
	☐ New	☐ Standard equipment supplied by a manufacturer ☐ CERN/collaboration responsible for the design and/or manufacturing
[Part 2 of experiment/ equipment]	☐ Existing	☐ To be used without any modification ☐ To be modified
	☐ New	☐ Standard equipment supplied by a manufacturer ☐ CERN/collaboration responsible for the design and/or manufacturing
[insert lines if needed]		

HAZARDS GENERATED BY THE EXPERIMENT (if using fixed installation:) Hazards named in the document relevant for the fixed CRIS installation.

Additional hazards: no additional hazards

Hazards	[Part 1 of experiment/ equipment]	[Part 2 of experiment/ equipment]	[Part 3 of experiment/ equipment]
Thermodynamic and fluidic			
Pressure	[pressure][Bar], [volume][l]		
Vacuum			
Temperature	[temperature] [K]		
Heat transfer			
Thermal properties of materials			
Cryogenic fluid	[fluid], [pressure][Bar], [volume][l]		
Electrical and electromagnetic			
Electricity	[voltage] [V], [current][A]		
Static electricity			
Magnetic field	[magnetic field] [T]		
Batteries	☐		
Capacitors	☐		

Ionizing radiation			
Target material [material]			
Beam particle type (e, p, ions, etc)			
Beam intensity			
Beam energy			
Cooling liquids	[liquid]		
Gases	[gas]		
Calibration sources:	□		
• Open source	□		
• Sealed source	□ [ISO standard]		
• Isotope			
• Activity			
Use of activated material:			
• Description	□		
• Dose rate on contact and in 10 cm distance	[dose][mSV]		
• Isotope			
• Activity			
Non-ionizing radiation			
Laser			
UV light			
Microwaves (300MHz-30 GHz)			
Radiofrequency (1-300 MHz)			
Chemical			
Toxic	[chemical agent], [quantity]		
Harmful	[chem. agent], [quant.]		
CMR (carcinogens, mutagens and substances toxic to reproduction)	[chem. agent], [quant.]		
Corrosive	[chem. agent], [quant.]		
Irritant	[chem. agent], [quant.]		
Flammable	[chem. agent], [quant.]		
Oxidizing	[chem. agent], [quant.]		
Explosiveness	[chem. agent], [quant.]		
Asphyxiant	[chem. agent], [quant.]		
Dangerous for the environment	[chem. agent], [quant.]		
Mechanical			

Physical impact or mechanical energy (moving parts)	[location]		
Mechanical properties (Sharp, rough, slippery)	[location]		
Vibration	[location]		
Vehicles and Means of Transport	[location]		
Noise			
Frequency	[frequency],[Hz]		
Intensity			
Physical			
Confined spaces	[location]		
High workplaces	[location]		
Access to high workplaces	[location]		
Obstructions in passageways	[location]		
Manual handling	[location]		
Poor ergonomics	[location]		

Hazard identification:

Average electrical power requirements (excluding fixed ISOLDE-installation mentioned above): [make a rough estimate of the total power consumption of the additional equipment used in the experiment]